ANNALS OF GEOPHYSICS, 61, 5, DA558, 2018; doi: 10.4401/ag-7852

"TESTING THE VALUE OF A MULTI-SCALE GRAVIMETRIC ANALYSIS IN CHARACTERIZING ACTIVE FAULT GEOMETRY AT HYPOCENTRAL DEPTHS: THE 2016-2017 CENTRAL ITALY SEISMIC SEQUENCE"

Paola Luiso[1], Valeria Paoletti[1,*], Rosa Nappi[2], Germana Gaudiosi[2], Federico Cella[3], Maurizio Fedi[1]

(1) Università degli Studi di Napoli Federico II, Dipartimento di Scienze della Terra, dell'Ambiente e delle Risorse, Napoli, Italy

(2) Istituto Nazionale di Geofisica e Vulcanologia, Sezione di Napoli - Osservatorio Vesuviano, Napoli, Italy

(3) Università della Calabria, Dipartimento di Biologia, Ecologia e Scienze della Terra, Arcavacata di Rende, Cosenza, Italy

Article history
Receveid **July 4, 2018**; accepted **October 14, 2018.**
Subject classification:
Multi-scale Gravimetric Analysis; Imaging Methods; Mt. Vettore-Mt. Bove.

ABSTRACT

We report the results of a multidisciplinary investigation performed across the normal Quaternary faults that ruptured the surface during the August 24 (M_w 6.0) and October 30 (M_w 6.5), 2016 strong earthquakes in the Mt. Vettore-Mt. Bove areas, central Italy. Our aim is to test the effectiveness of the contribution of a multi-scale gravimetric analysis in characterizing seismogenic faults' geometry at hypocentral depths on well-known outcropping faulty systems with known earthquake distribution. We adopted a multi-scale geophysical/geological approach consisting in the comparison of gravity lineaments inferred by *Multiscale Derivative Analysis* with the Quaternary structural setting mapped in the study area, the primary coseismic surface ruptures of the 2016-2017 sequence and the earthquakes' epicentral distribution. Moreover, we performed a combined interpretation of 2D hypocentral sections of the 2016-2017 seismic sequences with images resulting from the *Depth from Extreme Points* method, to infer the faults' geometry at depth. Based on our results, the investigated NW-SE Mt. Vettore-Mt. Bove fault system is dipping 60°-70° westward. We also detected the splays of this primary fault and its blind antithetic NW-SE structure, dipping northeastward. In the Norcia basin we highlight two main faults bordering the basin with a dip of about 45°. The one edging the eastern side dips westward, whereas the fault edging the western side dips eastward. Thanks to our analysis we could identify and characterize the geometry of the Norcia and Vettore master faults, as well as other blind/buried and/or silent faults that are related to the 2016 seismogenic structure. Our results show the effectiveness of this approach in potentially high-hazard areas that are structurally poorly known.

1. INTRODUCTION

Geological and geophysical techniques are important methods to characterize systems of active faults. The deep anatomy of fault zones is extremely complex, since they typically display strong lithological heterogeneity, physical discontinuity and textural anisotropy. Generally, only limited portions of active faults are exposed at the surface, for the combined result of erosion and tectonic rock exhumation. Instead, many faults are blind, i.e., they do not reach the surface. The tectonically active regions of the central Apennines are characterized by Quaternary segmented normal fault-systems with low strain-rates. These fault segments generated linear hanging wall mountain fronts and bounded footwall basins filled by thick clastic covers [Boncio et al., 2004; Roberts and Michetti, 2004; Porreca et al., 2016]. Important details of the active fault structure are hidden beneath those intermountain basins. This might make the signature of recent faulting difficult to read. Therefore, geological cross-sections providing subsurface characterization combined with geophysical investigation (e.g., seismic reflection data and deep-well logs) can yield effective solution for better investigating

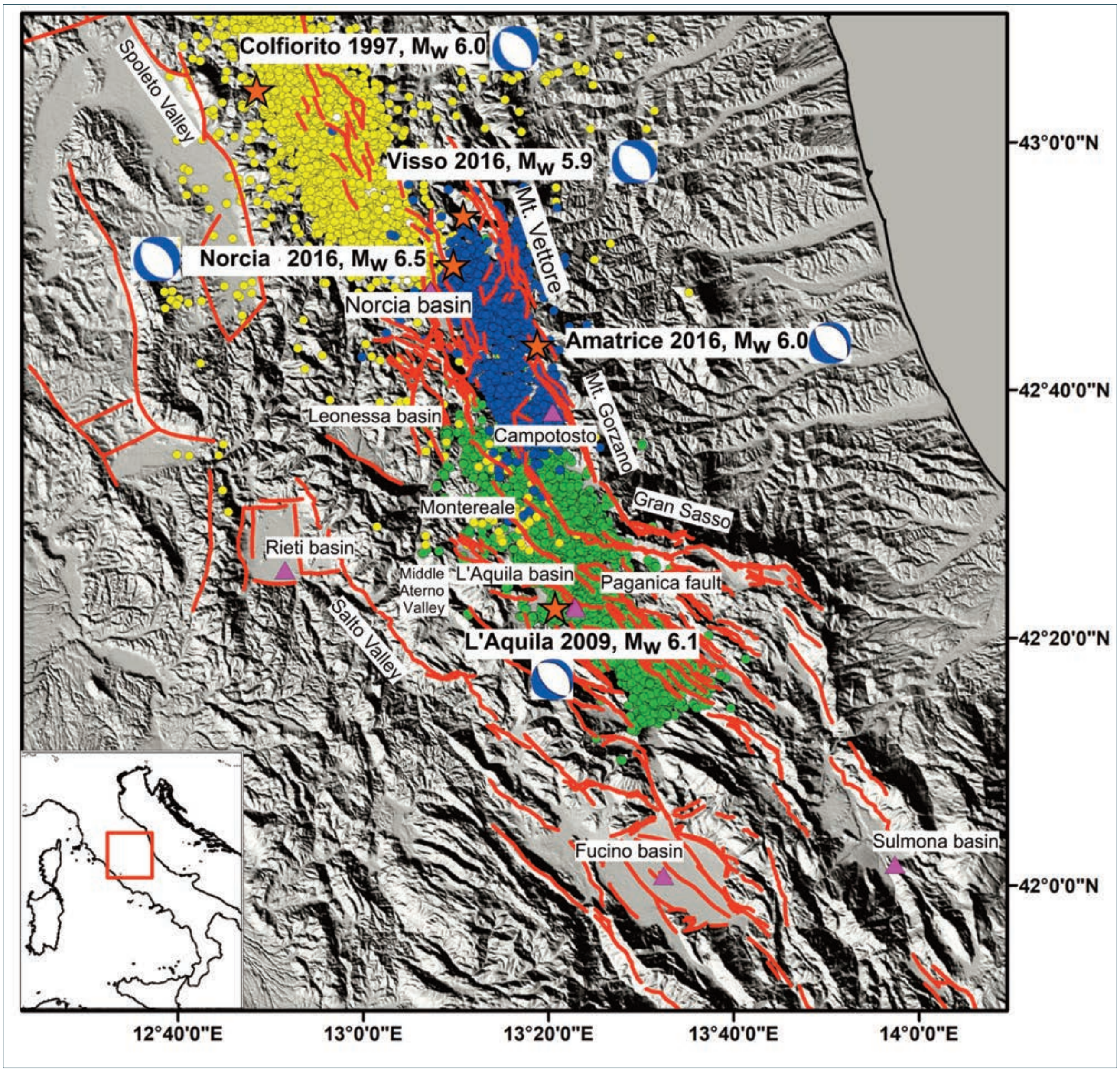

FIGURE 1. Central Apennines: Sketch of the main active normal faults extracted from literature (red lines) [Blumetti et al., 1993; Cinti et al., 1999; Galadini and Galli, 2000; Pizzi et al., 2002; Galadini and Galli, 2003; Boncio et al., 2004], the intra-mountain depressions (pink triangles) [Lavecchia et al., 2009] and the seismicity of the three main instrumental sequences of Central Apennines. Yellow dots: Colfiorito 1997-1998 sequence [Lavecchia et al., 2017]; green dots: L'Aquila 2009 sequence [Lavecchia et al., 2012]; blue dots: central Italy 2016-2017 sequence [Michele et al., 2016]; orange stars: main shocks; beach-balls: focal mechanisms of the three mainshocks of the seismic sequence and historical events [Istituto Nazionale di Geofisica e Vulcanologia- INGV].

active fault zones and the structure at the scale of the whole seismogenic crust. In fact, geological studies have the limit of investigating the shallowest kilometers of subsurface. Geophysical active methods (e.g., seismic reflection profiles and seismic/electrical 2D-tomography, or MASW - Multichannel Analysis of Surface Waves) and passive methods (measurements of Teleseismic P-waves and ambient noise) can yield important information on the subsoil characteristics and/or rupture planes [e.g., D'Amico et al., 2010; Panzera et al., 2016; Pischiutta et al., 2017]. Furthermore, the interpretation of gravity data alone [e.g., Paoletti et al., 2013], or in combination with stress-field data [e.g., Xu et al., 2015] has shown to be effective in retrieving information about active faults. A recent geophysical investigation, based on paleomagnetic and aeromagnetic data, provided an interpretation of the fault system in the Central Apennine area hit by destructive historical earthquakes including the 2009 L'Aquila seismic sequence [Minelli et al., 2008]. The study showed that the

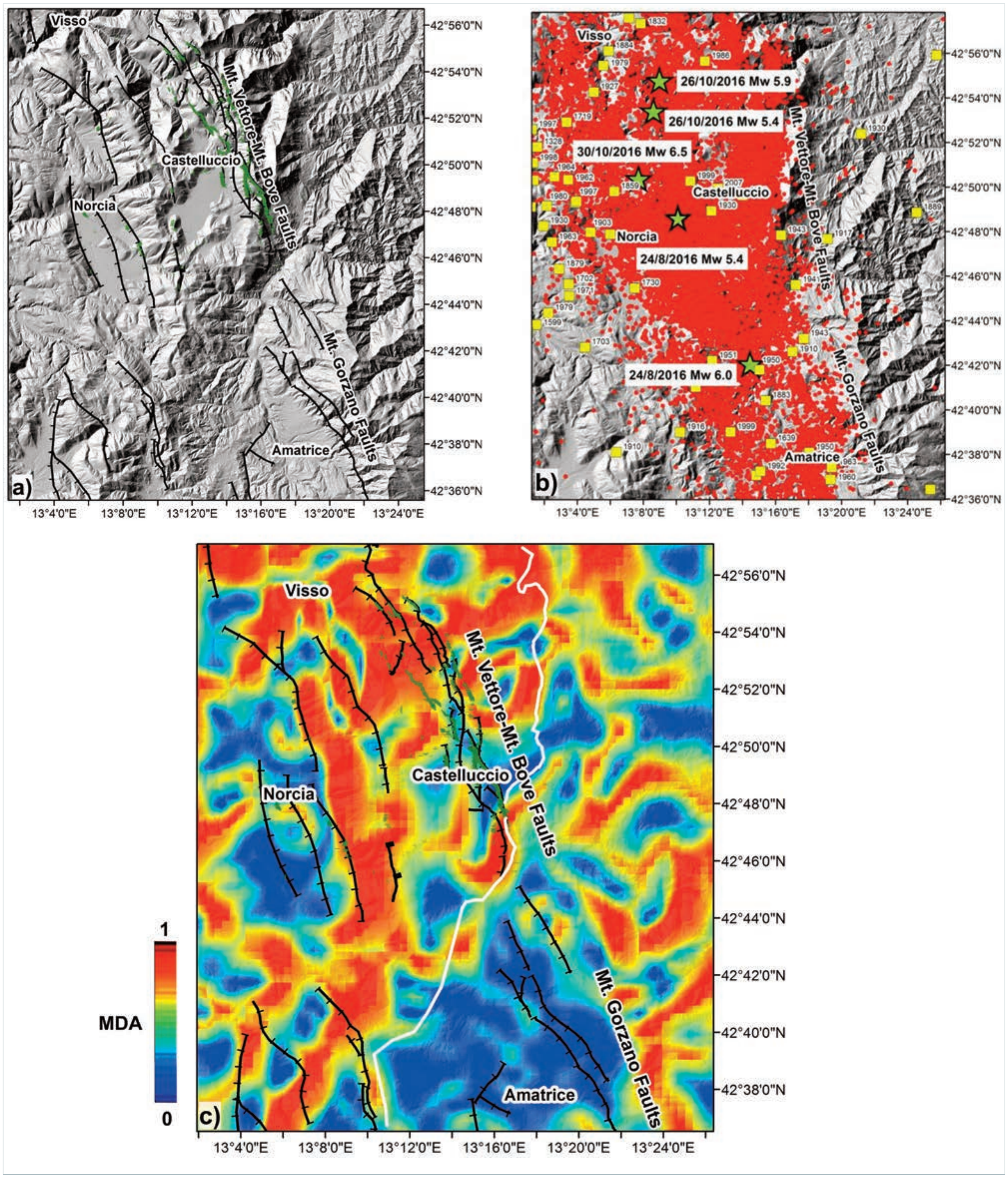

FIGURE 2. The three datasets used in this work: **a)** Structural dataset: the main active normal faults are from Blumetti et al. [1993], Galli et al. [2003], Galli et al. [2018] and references therein (black lines); primary coseismic ruptures from Civico et al. [2018] (green lines); **b)** Seismological dataset: relocated events from Michele et al. [2016] and Chiaraluce et al. [2017] (red dots); historical seismicity from CPTI15 [Rovida et al., 2016] (yellow squares); green stars are the strongest events of the 2016-2017 seismic sequence; **c)** Gravimetric dataset: MDA signal with main normal faults, primary coseismic ruptures and the Sibillini Thrust [Pizzi and Galadini, 2009] (white line).

boundaries of most prominent aeromagnetic anomalies are related to probable seismogenic faults formed after 0.7 Ma.

The 2016-2017 Amatrice-Visso-Norcia (Central Italy) seismic sequence caused primary surface faulting [Livio et al., 2016; Civico et al., 2018], which involved a com-

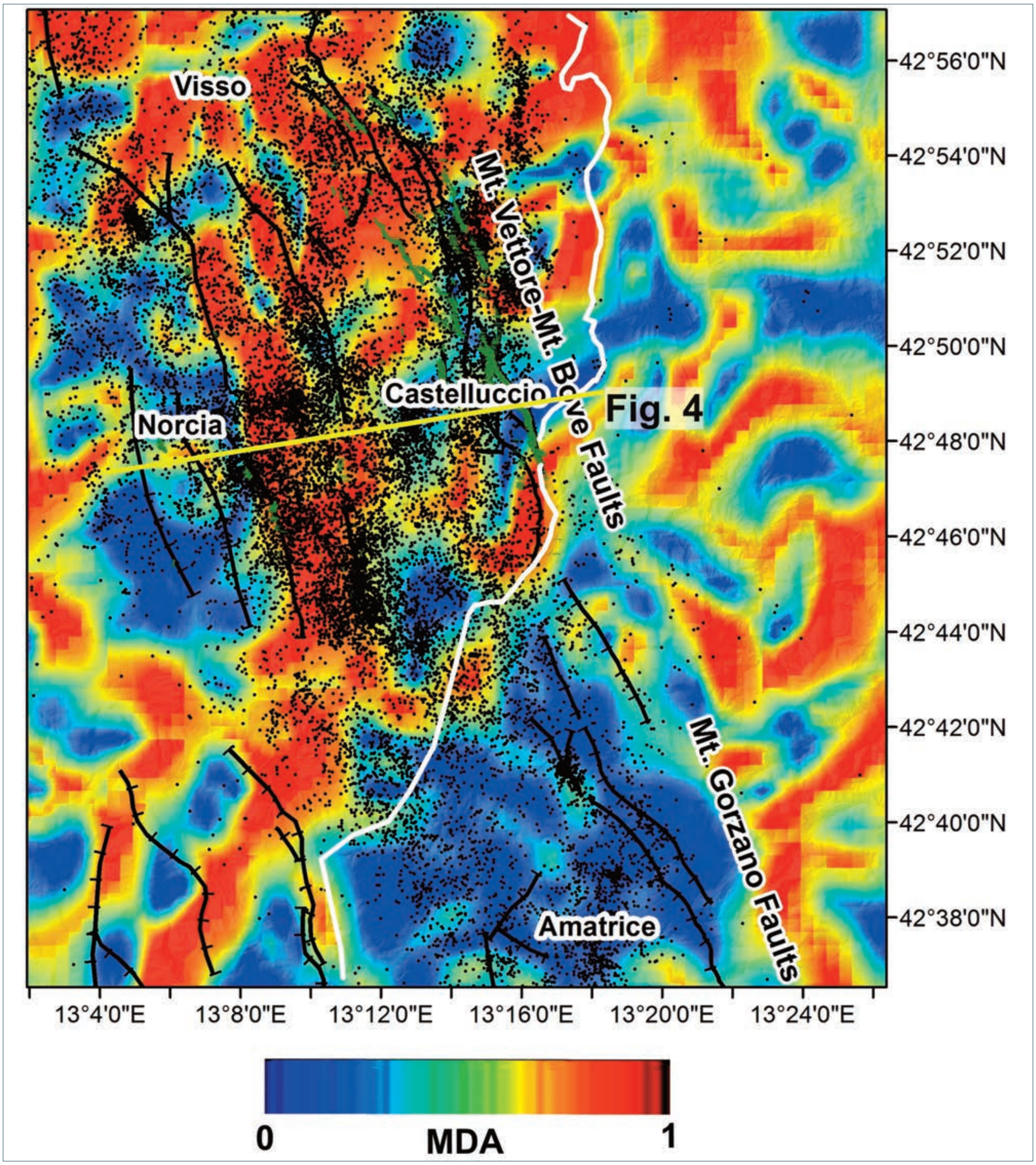

FIGURE 3. Merge of the structural, seismological and gravimetric datasets in the area of the Mt. Vettore-Mt. Bove and Norcia fault systems. Black lines: faults from literature (see text); green lines: primary coseismic ruptures [Civico et al., 2018]; white line: the Sibillini Thrust; black dots: earthquakes relocated by Michele et al. [2016] and Chiaraluce et al. [2017]. The yellow line shows the pattern of the section analysed in Figure 4.

plex network of normal fault segments. Most of these structural features have a clear geomorphic expression and directly expose limestone bedrock fault planes in high and rough mountainous areas. However, source models based on combined analysis of seismological and geodetic data clearly show that the structural complexity of the seismogenic volume played an important role in controlling the evolution of the earthquake sequence [e.g., Chiaraluce et al., 2017; Cheloni et al., 2017; Walters et al., 2018 and reference therein]. The seismological source model based on analysis of the space-time evolution of the seismic sequences shows the role of the inherited faults [Chiaraluce et al., 2017]. These faults, which separate different geological domains, seem to modulate the evolution of the sequence interfering with coseismic slip distribution and fault segments interaction. The analysis of the InSAR dataset and GPS measurements suggests, as well, a complex interaction in the activated crustal volume between the main normal faults and the secondary structures, and a partitioning of strain release [Cheloni et al., 2017]. The source model proposed by Walters et al. [2018] shows that the intersecting of major and subordinate faults controlled the extent and termination of rupture in each event in the sequence. Moreover, these same structural barriers may also be controlling the timing of failure in seismic sequences by channeling pressure-driven fluids flow along the fault planes.

Considering these interpretations, we investigate the Mt. Vettore-Mt. Bove and Norcia basin (Figure 1) by applying our methodology of analysis. We focus on the identification and interpretation of complex geologic structures/faults with density contrast, with the aim of recognizing the geometry at depth of the different faulty systems.

We use an integrated analysis of geo-structural, seismological and gravimetric data in GIS environment. We built three thematic datasets (Figure 2): the "fault dataset" consists of the collection of tectonic structures extracted from different catalogues and scientific papers; the "earthquake dataset" contains the instrumental and historical earthquakes from the available catalogues and datasets; the "gravimetric dataset" consists of lineaments identified by the *Multiscale Derivative Analysis* [MDA, Fedi, 2002] maxima of the Bouguer anomaly map. MDA is a valuable tool for the identification and interpretation of complex geologic structures/faults with density contrast. The horizontal correlation among gravimetric lineaments, earthquake epicentral distribution and faults/coseismic surface ruptures was integrated with an investigation of faults at depth in the areas of Mt. Vettore-Castelluccio and Norcia (Figure 3). To this aim, we used the *Depth from Extreme Points* method [DEXP, Fedi, 2007] that produces an image of the source density distribution with depth.

Our combined analysis of the DEXP images, primary coseismic ruptures, hypocentral sections of the 2016-2017 Amatrice-Visso-Norcia seismic sequence [Michele et al., 2016; Chiaraluce et al., 2017] and seismic sections [Porreca et al., 2018] allowed defining the geometry and depth extent across the faults of Mt. Vettore-Mt. Bove and the Norcia and Castelluccio basins, even though the sequence affected a much larger area up to the Campotosto fault. This multimethod approach is novel and was only recently applied to the faults bordering the Mt. Massico horst (Southern Italy) [Luiso et al., 2018]. Thus, here we also aim at testing the effectiveness of this multidisciplinary approach, and more specifically the contribution of multi-scale gravimetric analysis, in characterizing the geometry of the 2016-2017 seismic sequence causative faults at seismogenic depths.

2. SEISMOTECTONIC FRAMEWORK

The study area is characterized by a complex structural framework deriving from the interaction between pre-existing (Miocene-Pliocene) compressional structures (e.g., folds and thrusts due to the emplacement of the Apennine chain) and Quaternary extensional faults (due to post-orogenic collapse) [e.g., Calamita and Pizzi, 1994; Tavarnelli et al., 2004].

The Apennine Chain is an east-verging belt developed in Neogene times above a west-dipping subduction due to the convergence between the African and European Plates [Malinverno and Ryan, 1986; Doglioni, 1991; Cosentino et al., 2017]. The Sibillini Thrust is the major compressional structure of the region (Figure 2c). In the current extensional tectonic phase this thrust is activated as a steep structural barrier at depth to the main NW-SE striking normal faults [Pizzi and Galadini, 2009, Walters et al., 2018].

The eastward migration of the thrusts is associated with the opening of the back-arc extensional Tyrrhenian Sea basin [Patacca et al., 1990]. Since the late Miocene (for the northern Apennine), and the Early Pliocene (for the southern Apennine), the basin extended progressively to the east, causing the drowning of the internal sector of the orogenic wedge and the formation of coastal grabens (peri-Tyrrhenian basins) along the SW flank of the chain. During the Quaternary, the migration of the extension towards NE affected the Apennine chain axis generating normal fault systems consisting of NW to WNW trending and generally SW dipping segments responsible for major historical [Rovida et al., 2016] and instrumental earthquakes.

The Umbria-Marche-Abruzzo intra-Apennine extensional belt consists of three alignments of Quaternary normal and normal-oblique faults with NW-SE strike (Figure 1), named respectively: external (Mt. Vettore-Mt. Bove, Mt. Gorzano, Gran Sasso), intermediate (Gubbio, Colfiorito, Norcia, L'Aquila, the Middle Aterno Valley, Sulmona), and internal (Rieti, Salto Valley, Fucino, Barrea) [Boncio et al., 2004; Roberts and Michetti, 2004; Lavecchia et al., 2012]. These fault-systems controlled the formation of intermountain basins (the Rieti, Norcia, Leonessa, Colfiorito, Fucino, Sulmona and L'Aquila basins) (Figure 1). The depressions are filled with continental deposits of Plio-Quaternary age [Miccadei et al., 1997; Bosi et al., 2003; Cosentino et al., 2017].

Two major events with M_w > 5.5 occurred in the last 100 years: the one of Avezzano in 1915 with Ms 6.9 and the event of Barrea in 1984 with M_w 5.9. Four earthquakes hit the intermediate alignment: Gubbio 1984, M_w 5.6; Colfiorito 1997, M_w 6.0; Norcia 1979, M_w 5.9; L'Aquila 2009, M_w 6.1. No instrumental events with M_w > 4.5 were associated with the external alignment until the 2016 Amatrice seismic sequences with M_w= 6.5 (Figure 1).

More specifically, on August 24th, 2016, the M_w 6.0 Amatrice earthquake started a seismic sequence in central Apennines that lasted for months, causing numerous casualties and infrastructure damage [Galli et al., 2017]. The sequence included three mainshocks: the M_w 6.0 Amatrice earthquake, the M_w 6.1 event that occurred on October 26th 2016 and the M_w 6.5 Norcia earthquake that occurred on October 30th, 2016 (Figure 1). The M_w 6.5 earthquake is the largest event that struck Italy since the 1980 M_w 6.9 Irpinia earthquake.

These mainshocks have been accompanied by about eighty-five thousand aftershocks including five earthquakes with 5.4< M_w <5.9 [Chiaraluce et al., 2017]. The three mainshocks (M_w 6.1, 6.0 and 6.5) occurred at depths between ~7 and ~9 km along the Mt. Vettore-Mt. Bove fault's system [Lavecchia et al., 2017; Mildon et al., 2017; Walters et al., 2018].

Focal mechanisms of the three main events show a normal faulting plane 50° SW dipping and striking N150°. Such a main plane is interconnected at shallower depths with a set of synthetic and antithetic splays of different dimensions located both on the main fault's footwall and hanging wall. The entire fault system is constrained at about 7-8 km of depth by a 2-3-km-thick layer gently dipping to the east which was activated during the 2016-17 seismic sequence [Chiaraluce et al., 2017]. The seismic sequence was confined within the upper 10-12 km of the crust and the volume affected by the aftershocks extends for a distance of ~ 80 km, with NW-SE and NE-SW directions. The distribution of seismicity also suggests the activation of antithetic NE-dipping extensional faults.

The main active tectonic structures in the area affected by the 2016-2017 seismic sequence are the Mt. Vettore-Mt. Bove, the Mt. Gorzano-Campotosto (Laga fault system) and the Norcia-Montereale fault systems (Figure 1). The sequence occurred in the seismic gap between the 1997-98 Colfiorito seismic sequence (M_w 5.4 and M_w 5.9 earthquakes) and the 2009 L'Aquila earthquake (M_w 6.3). It was generated by Mt. Vettore-Mt. Bove and Laga fault systems (between Colfiorito and Campotosto areas) that represents the easternmost active extensional fault zones of the southern Umbro-Marchean Apennine ridge, characterized by normal to transtensive behaviour [Pizzi et al., 2009]. A portion of the Norcia system fault activated with the 30 October 2016 event.

The historical seismicity correlated with the most external fault system of the Umbria-Marche- Abruzzi Apennine ridge is characterized by absence of strong energy-seismicity along the Mt. Vettore-Mt. Bove sector, suggesting that the fault system was silent until the 2016 seismic sequence [Galadini and Galli, 2000], with the only exception of the Amatrice area in the hanging wall of the northern segment of the Mt. Gorzano fault, which ruptured during the October 1639 earthquake (M_w 5.9) [Rovida et al., 2016]. Geological and paleoseismological surveys [Galadini and Galli, 2003] showed that this central Apennines area of seismic gap could have potentially generated an earthquake of M_w = 6.5-7.0.

Coseismic ruptures of the 2016-2017 Amatrice-Norcia-Visso sequence were observed along several fault planes belonging to the main Mt. Vettore-Mt. Bove fault system, both on synthetic and antithetic splays (Figure 2a) with a complex N135°-160° (SW-dipping) surface faulting and a subordinate strike of N320°-345° (NE dipping) along about 28 km of the active fault system. Moreover, very discontinuous ruptures affected the SW edge of the Castelluccio di Norcia (hereafter "Castelluccio") basin and the Norcia area [Civico et al., 2018].

3. METHOD

We carried out our study by the collection and comparison of seismicity, faults and gravimetric lineaments, in GIS environment. This allowed us to identify the possible active faults and to pick up the more interesting structures to be studied through a 2D analysis. More specifically:

- The "fault datasets" (Figure 2a) consists of the collection of tectonic structures extracted from literature [Centamore et al., 1992; Blumetti et al., 1993; Cinti et al., 1999; Galadini and Galli, 2000; Pizzi et al., 2002; Galli et al., 2003; Boncio et al., 2004; Galli et al., 2008; Pierantoni et al., 2013] and the primary coseismic ruptures of the Amatrice-Norcia-Visso 2016-2017 seismic sequences [Civico et al., 2018]. These structures were organized in a vector database. An attribute table accompanies the datasets containing, for each fault, relevant information such as: ID number, Name, Type, Age, Dip, Length, Direction, Geographic Coordinates, References and Correlation with Topography.

- The "earthquake datasets" (Figure 2b) consists of seismic data extracted from the CPTI15 Catalogue of Parametric Italian Earthquakes [Rovida et al., 2016] containing the earthquakes locations from year 1000 to 2014 A.D., and focal mechanism from the Istituto Nazionale di Geofisica e Vulcanologia (INGV) of Italy. The instrumental seismicity of the study area was extracted from the ISIDE database (Italian Seismological Instrumental and Parametric Database) containing all Italian earthquakes since 1985 A.D.. The aftershocks location of the Amatrice-Norcia-Visso sequence derived from Michele et al. [2016] and Chiaraluce et al. [2017].
- The "gravimetric datasets" (Figure 2c) is made of data deriving from the *Multiscale Derivative Analysis* [MDA, Fedi, 2002] of the Bouguer Gravity Anomaly Map of Italy published by CNR [Carrozzo et al., 1986]. The gravimetric data, with sampling rate of 1 km, were obtained using a Bouguer reduction density of 2.4 g/cm^3. The gravity anomaly field of central Apennines, obtained after gridding data to an interval of 0.5 km, shows the presence of negative and positive short-wavelength anomalies, superimposed to regional ones. The latter are represented by an elongated low running along the main axis of the Apennine chain and by an extended high, whose maxima is in the central area of the Tyrrhenian basin. Our use of the MDA edge analysis tool (see Section 3.1) is justified by the complexity of the geology in the Apennine chain where many sources related to different depths and extents contribute the measured anomalies.

3.1 MULTISCALE DERIVATIVE ANALYSIS

Multiscale Derivative Analysis [Fedi et al., 2005] is based on the properties of the Enhanced Horizontal Derivative signal [EHD, Fedi and Florio, 2001], a high-resolution multiscale edge estimator.

The EHD is based on the horizontal derivative of a weighted sum of any-order derivative of the gravity or magnetic potential:

$$EHD(x,y) = \sqrt{\left(\frac{\partial \phi}{\partial x}\right)^2 + \left(\frac{\partial \varphi}{\partial y}\right)^2} \qquad (1)$$

where:

$$\phi(x,y) = w_0 f(x,y) + w_1 f^{(1)}(x,y) + w_2 f^2(x,y) + \dots w_m f^{(m)}(x,y) \qquad (2)$$

and $f^{(m)}(x,y)$ is the m-order derivative of the potential and $w_0 \ldots w_m$ are the set of weights that control the relative influence of the single terms in the summation. Better details of the shallow sources are obtained by adding higher-order derivative terms. The use of the highest order derivatives is in practice limited by the data-sampling step (1 km for the analyzed data set). As sources of different depth/extent generate effects at various scales, different images of the source edges can be obtained by appropriately choosing the first and last terms of the summation (2). The MDA method does not apply sharp component separation (as filtering does) but enhances the contributions with a different resolution/scale contained in the data, based on the m-order derivative of the summation (2) [Fedi et al., 2005]. The source boundaries and/or faults contacting lithologies with different densities are emphasized as maxima of the EHD signal. These maxima are located above the lineaments in the case of vertical boundaries/faults. In the case of faults dipping with a low angle (e.g. 45-60°), there is a shift between the position of the fault and its MDA maximum.

The MDA map shown in Figure 2c was obtained by considering the gravity field and its vertical gradient up to the 5th order (medium scale) which was found - based on our tests - to optimally highlight the medium scale structures of the area. The correlation between faults, primary coseismic ruptures, earthquakes and MDA lineaments of the study areas was analysed for identifying potentially active, outcropping, buried and/or silent faults. We note that the presence of topographic highs may influence the MDA maxima. For this reason, it is important to study the source of each MDA maximum with the support of seismicity. Thus, we created an attribute table in which, for each lineament, we reported: i) ID number; ii) Correlation with topography; iii) Correlation with mapped faults; iv) Correlation with earthquakes; v) Notes: some comments about the correlations are made, e.g., if the MDA lineament crops out a topographic high or a seismic clustering perpendicularly; or, if the MDA lineament is only partially correlated with topography or earthquakes.

3.2 DEPTH TO EXTREME POINTS

To study the geometry and depth extent of some main faults of the area, we combined a multiscale analysis on gravity data with information derived from hypocentral sections. The gravity multiscale analysis was performed through the *Depth from Extreme Points* method [DEXP, Fedi, 2007; Fedi and Pilkington, 2012] that is a fast technique for analysis of potential fields yielding a 3D image of the source distribution. The DEXP transformation is given by:

$$\Omega(\mathbf{r}, z_i) = T(\mathbf{r}, z_i)\,|z_i|^{N/2} \qquad i = 1, \ldots L, \qquad (3)$$

where $\Omega\ (\mathbf{r}, z_i)$ is the DEXP-scaled field at the altitude z_i, $T\ (\mathbf{r}, z_i)$ is the field T upward continued at z_i, and $|z_i|^{N/2}$ is the DEXP power-law of altitudes, having the source-dependent exponent $N/2$ (with N being the source structural index). The structural index N may be estimated through well-known methods such as *Euler Deconvolution* [e.g., Nabighian and Hansen 2001] or through multiscale methods such as the *Multiridge Euler Deconvolution* [e.g., Florio and Fedi 2013] and *Scaling Function Method* [e.g., Florio et al., 2009]. For complex cases, a reasonable N may be chosen as the one yielding source-density distributions consistent with known geological/geophysical information [Paoletti et al., 2014 and references therein].

Fedi [2007] showed that the extrema in the function Ω correspond to source locations, with the source depth given by the negative of the extreme point altitudes. Thus, we can make the substitution $h_i=|z_i|$ in Equation (3) and obtain the DEXP image $\Omega\ (\mathbf{r}, h_i)$ within the source domain. For positive contrasts of density (or magnetization), the extreme value is a maximum, and for negative properties, the extreme value is a minimum. The method is applied to vertical or horizontal derivatives of the gravity/magnetic field, with the differentiation being performed through the *Integrated Second Vertical Derivative* (ISVD) procedure [Fedi and Florio, 2001] for the vertical derivatives, in the space-domain for the horizontal derivates and through the Fourier Transform for the upward continuation.

As DEXP is a physically-based transformation mainly consisting of upward continuation and differentiation, it can decrease interference effects and infer the depth of the source-distribution without any pre-filtering [e.g., Paoletti et al., 2016]. This yields consistent and stable results even when using high-order derivatives of the field and with a low signal/noise ratio.

Before using the DEXP method, we have continued the gravimetric data upward to 10 km a.s.l., with the aim of comparing the DEXP images and hypocentral sections, and we considered the horizontal gradient of the 4th vertical gradient of the gravimetric field. We combined the DEXP results with the information deriving from the re-located aftershocks provided by Michele et al. [2016].

4. RESULTS

The correlation between faults, earthquakes and MDA lineaments of the study areas was analysed in GIS environment (Figure 3) for identifying active, silent and inactive faults. We depicted two scenarios of correlation between our datasets in the studied region:

- A correlation between MDA maxima, known geological features and earthquake clustering [Michele et al., 2016] suggests the existence of active faults, e.g., in the Mt. Vettore-Mt. Bove and Castelluccio areas. The pattern of the MDA signal over the Mt. Vettore-Mt. Bove system of faults is rather complex, likely due to the presence of many fault splays with small length whose gravimetric signals influence each other. The two westernmost mapped faults of the Norcia plain are correlated with discontinuous MDA maxima and with earthquake swarms mainly located along the easternmost fault of the basin. The region from Mt. Vettore-Mt. Bove to Norcia was better investigated by constraining the faults' geometry at depth through the DEXP imaging method;
- A correlation between faults and earthquake swarms, but without MDA maxima suggests lack of density contrasts between the different lithologies along the faulty systems, e.g., the northern sector of the Gorzano fault system.

The map also shows a remarkable lateral density contrast along the Sibillini Thrust, even though with a discontinuous series of MDA maxima. Our analysis revealed that MDA signal is not influenced by topography in this area and thus the maxima must be related to underground tectonic features such as faults and/or thrusts.

Moreover, we performed a multiscale imaging of gravity data by the DEXP method along a profile about 25 km long crossing the Norcia and Castelluccio basins and Mt. Vettore-Mt. Bove (Figures 3,4). Then we combined the DEXP results with the information from hypocentral sections obtained using re-located aftershocks [Michele et al., 2016; Chiaraluce et al., 2017] and from deep geological sections [Porreca et al., 2018]. The latter proposed a reconstruction of the subsurface geology of the area close to the Norcia M_w 6.5 mainshock (30 October 2016) based on industrial seismic reflection profiles and available geological data, and found that most of seismicity is confined within the Meso-Cenozoic sedimentary sequence at depths of 8 to 11 km.

As hypocenters show a cluster down to about 10 km, we continued the gravimetric data upward to 10 km a.s.l., with the aim of comparing the DEXP images and the hypocentral sections. We considered the DEXP image of the modulus of the horizontal gradient of the 4th vertical

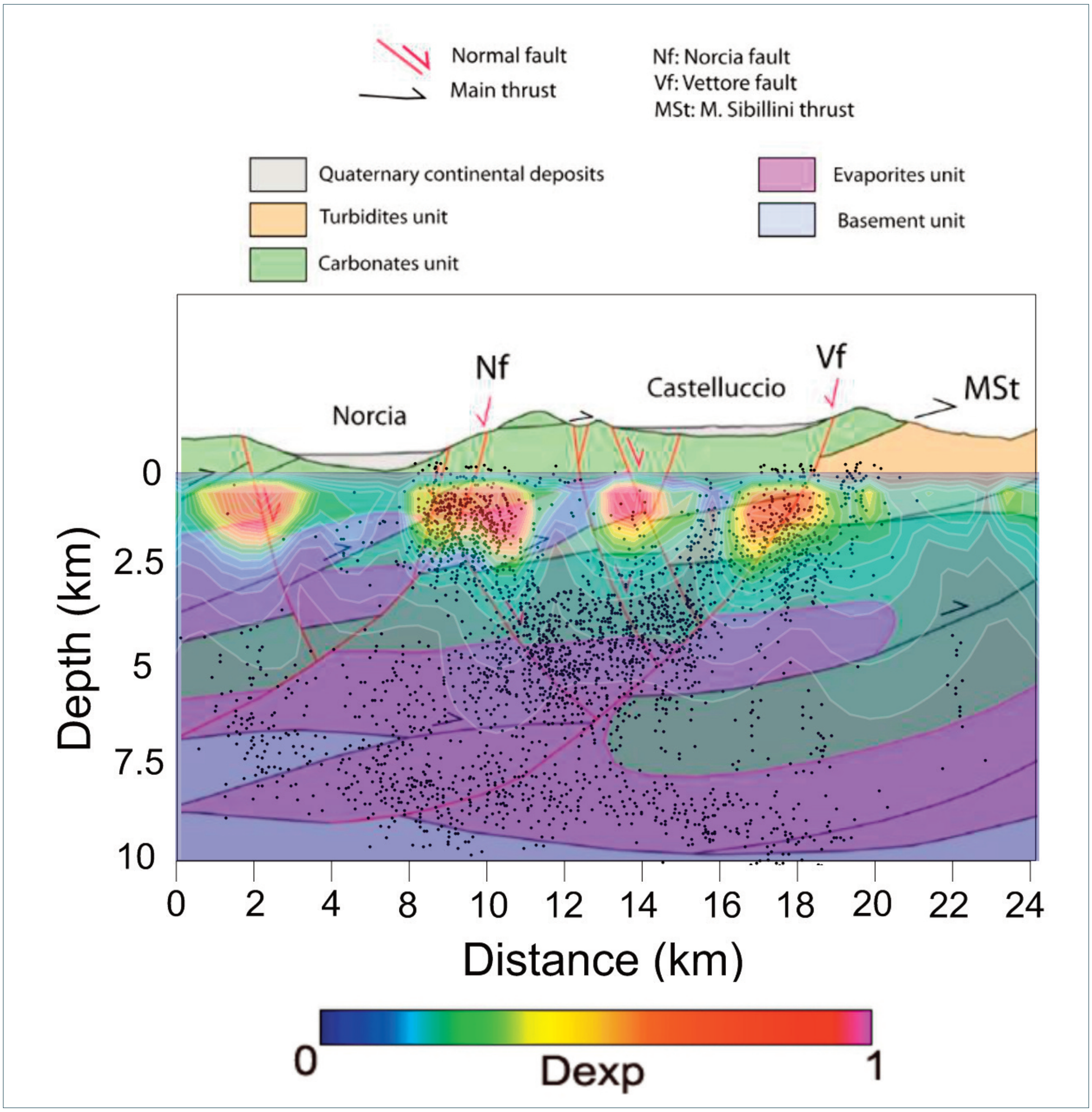

FIGURE 4. Combined analysis of the DEXP image and seismological data across the Norcia and Castelluccio basins and Mt. Vettore-Mt. Bove faulty system. Our analysis is overlaid to the seismic and geological section from Porreca et al. [2018]. The DEXP image shows five main highs that indicate the depth to the top of the major normal fault planes (about 1 km depth) controlling the seismic sources of the study area. The DEXP maxima show different patterns for the identified faults. For the DEXP, normalized dimensionless units are used.

derivative of gravity data. For both faults, we employed a structural index $N = -1$, based on known information on contact-like structures. The DEXP maxima are at about the depth-to-the-top of the fault plane, and the area covered by the DEXP highs is oriented similarly to the faults' dip.

The section deriving from our multi-scale imaging highlights five main maxima (Figure 4). The one below the peaks of Mt. Vettore is about 70° SW dipping and is well-matching with the main Mt. Vettore-Mt. Bove fault system as imaged by Porreca et al. [2018] and the hypocentral distribution. The DEXP maximum below Castelluccio shows a sub-vertical pattern in agreement with minor seismicity and with the system of faults imaged by seismic data. We note that the gravimetric data spacing of our dataset (1 km) does not allow clearly depicting fault planes that are very close to each other. In the central section of our profile the DEXP image shows two diverging maxima; one matches with the antithetic blind fault of Mt. Vettore dipping Eastwards and is accompanied by clustered seismicity. The other DEXP maximum is connected to the Norcia fault system, dipping

45° Westwards and with a clear hypocentre clustering. Finally, another maximum correlates with the Norcia antithetic fault dipping 45° Eastwards and is not accompanied by seismicity.

5. CONCLUSIONS

The aim of this paper is to test the contribution of a multi-scale gravimetric analysis in characterizing the faults' geometry from the surface to hypocentral depths and in validating our multi-scale geological/geophysical approach. It consists of the comparison of gravity lineaments inferred by *Multiscale Derivative Analysis* with the Quaternary structural setting mapped in the study area, the primary coseismic surfaces of the 2016-2017 sequence and the earthquakes' epicentral distribution. The MDA maxima highlight the source boundaries and/or faults contacting lithologies with different density. In the case of faults dipping with a low angle, such as thrusts and blind faults, a shift between the position of the fault and its MDA maximum may be observed. The major structure of the Sibillini Thrust, interpreted by several authors [Chiaraluce et al., 2017; Cheloni et al., 2017; Walters et al., 2018 and reference therein] as a controlling factor for rupture propagation and/or barrier during the earthquake sequence, was well-shown by the MDA signal (Figure 3).

We depicted different scenarios of correlation between faults, earthquakes and MDA maxima. The areas characterized by a good correlation between MDA maxima, known geological features and earthquake clustering were better investigated by constraining the fault geometry at depth applying the DEXP imaging method combined with 2D hypocentral sections [Michele et al., 2016; Chiaraluce et al., 2017], and reflection seismic and balanced cross-sections [Porreca et al., 2018]. Our analysis (Figure 4) shows a DEXP maximum below Mt. Vettore-Mt. Bove depicting a fault plane dipping 70° westward that matches well with the hypocentral distribution and the normal seismogenic faults reported in the literature [e.g., Cheloni et al., 2017; Porreca et al., 2018]. Moreover, the fault plane shown by DEXP corresponds at the surface with coseismic ruptures [Civico et al., 2018] that were activated, along the western margin of Mt. Vettore-Mt. Bove, by the M_w 6.0 and M_w 6.5 main shocks. We also detected a DEXP maximum below Castelluccio characterized by poor seismicity and matching with the system of faults imaged by seismic data. The gravimetric data spacing of our dataset does not allow clearly depicting fault planes that are very close to each other. Moving westwards along the profile, we observe a DEXP maximum dipping E-NE below the eastern margin of the Norcia basin and matching with the hypocentral distribution. This fault, not showing geological signature at surface, acts as the antithetic fault of the Mt. Vettore-Mt. Bove synthetic fault. A fourth DEXP maximum, dipping 45° W-SW, is in correspondence with the well-known fault edging the Norcia basin to the East and is also imaged by earthquake hypocentral distribution (Figure 4). The western-most DEXP maximum, corresponding with an E-NE dipping fault mapped at surface, is characterized by a scarce and sparse seismicity, testifying that this structure was likely non-active during the 2016-2017 seismic sequence.

In conclusions, our multi-scale gravimetric analysis allowed identifying: a) the primary Mt. Vettore-Mt. Bove fault of the 2016-2017 sequence, SW dipping; b) the antithetic fault of the Mt. Vettore-Mt. Bove fault system that activated during the seismic sequence; this antithetic fault is buried, i.e., it has no geological signature at the surface; c) the synthetic Norcia fault that also activated during the seismic sequence; d) a silent fault bordering the western margin of the Norcia basin, well-known in the geological literature.

Our imaging results showed to match rather well with the different fault systems known from geological and geophysical studies, similarly to what seen in the study by Minelli et al. [2018].

The major outcome of our study is that:

1) it was successfully tested in an area where the available seismological, seismic and geologic data are of excellent quality;
2) this approach was able to provide useful constrain to the geometry of the causative faults at hypocentral depths, even though the resolution of gravimetric data is in the order of 1 km.

Thus, we point out the effectiveness of our multi-parametric approach to constrain the fault plane geometry of known active structures in high-seismic-hazard areas. Moreover, the good agreement between the pattern of the DEXP maxima and aseismic faults (e.g., the westward fault on the Norcia basin), allows us to employ this new method also to identify buried and/or silent faults, especially in the areas where the sole seismological/structural analysis is not enough, or areas that are structurally poorly known.

Acknowledgements. The authors are grateful to the Associate Editor Fabio Caratori Tontini and to Alessandro Maria Michetti and an anonymous reviewer for their constructive comments.

REFERENCES

Blumetti, A.M., F. Dramis and A.M. Michetti (1993). Fault generated mountain fronts in the Central Apennines (Central Italy): geomorphological features and seismotectonic implications, Earth Surface Processes and Landforms, 18, 203-223.

Boncio, P., G. Lavecchia, and B. Pace (2004). Defining a model of 3D seismogenic sources for Seismic Hazard Assessment applications: The case of central Apennines (Italy), Journal of Seismology, 8, 407-425.

Bosi, C., P. Messina, and M. Moro (2003). Nuovi procedimenti cartografici per il Quaternario continentale: l'esempio della carta geologica dell'alta Valle dell'Aterno. Il Quaternario, 1166(1), 127-138.

Calamita, F. and A. Pizzi (1994). Recent and active extensional tectonics in the southern umbromarchean Apennines (central Italy). Memorie della Società Geologica Italiana, 48, 541-548.

Carrozzo, M.T., A. Chirenti, D. Luzio, C. Margiotta and T. Quarta (1986). Carta gravimetrica d'Italia. Acts of 5° Congress GNGTS, 2, 913-918.

Cheloni, D., V. De Novellis, M. Albano, A. Antonioli, M. Anzidei, S. Atzori, A. Avallone, C. Bignami, M. Bonano, S. Calcaterra, R. Castaldo, F. Casu, G. Cecere, C. De Luca, R. Devoti, D. Di Bucci, A. Esposito, A. Galvani, P. Gambino, R. Giuliani, R. Lanari, M. Manunta, M. Manzo, M. Mattone, A. Montuori, A. Pepe, S. Pepe, G. Pezzo, G. Pietrantonio, M. Polcari, F. Riguzzi, S. Salvi, V. Sepe, E. Serpelloni, G. Solaro, S. Stramondo, P. Tizzani, C. Tolomei, E. Trasatti, E. Valerio, I. Zinno and C. Doglioni (2017). Geodetic model of the 2016 Central Italy earthquake sequence inferred from InSAR and GPS data, Geophys. Res. Lett., 44, 6778-6787.

Chiaraluce, L., R. Di Stefano, E. Tinti, L. Scognamiglio, M. Michele, E. Casarotti, M. Cattaneo, P., De Gori, C. Chiarabba, G. Monachesi, A. Lombardi, L. Valoroso, D. Latorre and S. Marzorati, S. (2017). The 2016 Central Italy seismic sequence: a first look at the mainshocks, aftershocks, and source models. Seismological Research Letters, 88(3), 757-771. Doi: 10.1785/0220160221.

Centamore, E., L. Adamoli, D. Berti, G. Bigi, S. Bigi, R. Casnedi, G. Cantalamessa, F. Fumanti, C. Morelli, A. Micarelli, M. Ridolfi and R. Salvucci (1992). Carta geologica dei bacini della Laga e del Cellino e dei rilievi carbonatici circostanti. In: Studi Geologici Camerti, Spec. Vol. Università degli Studi, Dipartimento di Scienze della Terra. SELCA, Firenze.

Cinti, F.R., L. Cucci, F. Marra and P. Montone (1999). The 1997 Umbria-Marche (Italy) earthquake sequence: Relationship between ground deformation and seismogenic structure, Geophys. Res. Lett., 26, 895-898. Doi: 10.1029/1999GL900142.

Civico, R., S. Pucci, F. Villani, L. Pizzimenti, P.M. De Martini, R. Nappi, R. and Emergeo Working Group (2018). Surface ruptures following the 30 October 2016 M_w 6.5 Norcia earthquake, central Italy. Journal of Maps, 14(2), 151-160. Doi: 10.1080/17445647.2018.1441756.

Cosentino, D., R. Asti, M. Nocentini, E. Gliozzi, T. Kotsakis, M. Mattei, M. Pennacchioni, G. Cavuoto and V. Di Fiore (2017). New insights into the onset and evolution of the central Apennine extensional intermontane basins based on the tectonically active L'Aquila Basin (central Italy). Geological Society of America Bulletin, 129(9-10), 1314-1336. doi.org/10.1130/B31679.1.

D'Amico, S., K.D. Koper, R.B. Herrmann, A. Akinci and L. Malagnini (2010). Imaging the rupture of the M_w 6.3 April 6, 2009 L'Aquila, Italy, earthquake using back-projection of teleseismic P-waves. Geophysical Research Letters, 37(3): L03301. Doi:10.1029/2009GL042156.

Doglioni, C. (1991). A proposal of kinematic modelling for W-dipping subductions-possible applications to the Tyrrhenian-Apennines system. Terra Nova, 3(4), 423-434. Doi: 10.1111/j.1365-3121.1991.tb00172.x.

Fedi, M. and G. Florio (2001). Detection of Potential fields source boundaries by Enhanced Horizontal Derivative method. Geophysical Prospecting, 49(1), 40-58. Doi:10.1046/j.1365-2478.2001.00235.x.

Fedi, M. (2002). Multiscale Derivative Analysis: a new tool to enhance gravity source boundaries at various scales. Geophysical Research Letters, 29, 16-1-16-4. Doi:10.1029/2001GL013866.

Fedi, M., F. Cella, G. Florio, and A. Rapolla, A. (2005). Multiscale Derivative Analysis of the gravity and magnetic fields of the Southern Apennines (Italy). In: Finetti I.R. (ed), CROP PROJECT: Deep Seismic Exploration of the Central Mediterranean and Italy, 281-318.

Fedi, M. (2007). DEXP: A fast method to determine the depth and the structural index of potential fields sources. Geophysics, 72(1), 1-11. Doi:org/10.1190/1.2399452.

Fedi, M., and M. Pilkington (2012). Understanding imaging methods for potential field data. Geophysics, 77, G13-G24. Doi: 10.1190/geo2011-0078.1.

Florio, G., M. Fedi and A. Rapolla, A. (2009) Interpretation of regional aeromagnetic data by the scaling function method: the case of Southern Apennines (Italy), Geophys. Prospect., 57(4), 479-489.

Florio, G. and M. Fedi (2014). Multiridge Euler deconvolution, Geophys. Prospect., 62(2), 333-351. Doi:10.1111/1365-2478.12078.

Galadini, F. and P. Galli (2000). Active tectonics in the Central Apennines (Italy) - input data for seismic hazard assessment. Natural Hazard, 22(3), 225-270. Doi: 10.1023/A:1008149531980.

Galadini, F. and P. Galli (2003). Paleoseismology of silent faults in the Central Apennines (Italy): the Mt. Vettore and Laga Mts. Faults. Annals of Geophysics, 46(5), 815-836. Doi: 10.4401/ag-3457.

Galli, P., F. Galadini and D. Pantosti (2008). Twenty years of paleoseismology in Italy. Earth-Science Reviews, 88, 89-117.

Galli, P., S. Castenetto and E. Peronace (2017). The macroseismic intensity distribution of the 30 October 2016 earthquake in central Italy (M_w 6.6): Seismotectonic implications. Tectonics, 36, 2179-2191. Doi: 10.1002/2017TC004583.

Galli, P., A., Galderisi, I. Ilardo, S. Piscitelli, V. Scionti, J. Bellanova and F. Calzoni (2018). Holocene paleoseismology of the Norcia fault system (Central Italy), Tectonophysics, 745, 154-169. Doi: 10.1016/j.tecto.2018.08.008.

INGV - Istituto Nazionale di Geofisica e Vulcanologia, Centro Nazionale Terremoti. Available online: http://cnt.rm.ingv.it/en (accessed on 12 March 2017).

Lavecchia, G., P. Boncio, F. Brozzetti, R. Nardis, D. Di Naccio, F. Ferrarini, A. Pizzi and G. Pomposo, (2009). The April 2009 L'Aquila (Central Italy) Seismic Sequence (M_w 6.3): a Preliminary Seismotectonic Picture. Recent Progress on Earthquake Geology, 1-17.

Lavecchia, G., F. Ferrarini, F. Brozzetti, R. de Nardis, P. Boncio and L. Chiaraluce (2012). From surface geology to aftershock analysis: constraints on the geometry of the L'Aquila 2009 seismogenic fault system. Italian Journal of Geosciences, 131, 330-347.

Lavecchia, G., G. Adinolfi, M. De Nardis, F. Ferrarini, D. Cirillo, F. Brozzetti, R. De Matteis, G. Festa, and A. Zollo (2017). Multidisciplinary inferences on a newly recognized active east-dipping extensional system in Central Italy. Terra Nova, 29, 77-89. Doi: 10.1111/ter.12251.

Livio, F.A., A.M. Michetti, E. Vittori, L. Gregory, L. Wedmore, L. Piccardi, E. Tondi, G. Roberts, CENTRAL ITALY EARTHQUAKE W.G., A.M. Blumetti, L. Bonadeo, F. Brunamonte, V. Comerci, P. Dimanna, M.F. Ferrario, J. Faure Walker, C. Frigerio, F. Fumanti, L. Guerrieri, F. Iezzi, G. Leoni, K. McCaffrey, Z. Mildon, R. Phillips, E. Rhodes, R.J. Walters and M. Wilkinson (2016.) Surface faulting during the August 24, 2016, Central Italy earthquake (M_w 6.0): preliminary results. Annals of Geophysics, 59, FAST TRACK 5, 8 pp. Doi: 10.4401/ag-7197.

Luiso, P., V. Paoletti, R. Nappi, M. La Manna, F. Cella, G. Gaudiosi, M. Fedi and M. Iorio (2018). A multidisciplinary approach to characterize the geometry of active faults: the example of Mt. Massico, Southern Italy. Geophysical Journal International, 213, 1673-1681. Doi: 10.1093/gji/ggy080.

Malinvemo, A. and W.B.F. Ryan (1986). Extension in the Tyrrhenian Sea and shortening in the Apennines as result of arc migration driven by sinking of the lithosphere. Tectonics, 5(2), 227-245. Doi:10.1029/TC005i002p00227.

Miccadei, E., R. Barberi and G. De Caterini (1997). Nuovi dati geologici sui depositi quaternari della Conca Subaequana (Appennino abruzzese). Il Quaternario, 10, 483-486.

Michele, M., R. Di Stefano, L. Chiaraluce, M. Cattaneo, P. De Gori, G. Monachesi, D. Latorre, S. Marzorati, L. Valoroso, C. Ladina, C. Chiarabba, V. Lauciani and M. Fares (2016). The Amatrice 2016 seismic sequence: A preliminary look at the mainshock and aftershocks distribution. Annals of Geophysics, 59, 1-8. Doi: 10.4401/ag-7227.

Mildon, Z.K., G.P. Roberts, J.P.F. Walkerand and F. Iezzi (2017) Coulomb stress transfer and fault interaction over millennia on non-planar active normal faults: the M_w 6.5-5.0 seismic sequence of 2016-2017, central Italy. Geophysical Journal International, 210(2), 1206-1218.

Minelli L., F. Speranza, I. Nicolosi, F.D. Caracciolo, R. Carlucccio, S. Chiappini, A. Messina, M. Chiappini (2018). Aeromagnetic Investigation of the Central Apennine Seismogenic Zone (Italy): From Basins to Faults, Tectonics, 37(5), 1435-1453.

Nabighian, M.N. and R.O. Hansen (2001). Unification of Euler and Werner deconvolution in three dimensions via the generalized Hilbert transform, Geophysics, 66, 1805-1810.

Panzera, F., G. Lombardo and C. Monaco (2016). New evidence of wavefield polarization on fault zone in the lower NE slope of Mt. Etna. Italian Journal of Geoscience, 135(2), 250-260. Doi: 10.3301/IJG.2015.22.

Paoletti, V., S., Ialongo, G. Florio, M. Fedi and F. Cella (2013). Self-constrained inversion of potential field. Geophysical Journal International, 195, 854-869. Doi: 10.1093/gji/ggt313.

Paoletti, V., P.C. Hansen, M.F. Hansen and M. Fedi (2014). A Computationally efficient tool for assessing the depth resolution in potential field inversion, Geophysics, 79(4), A33-A38.

Paoletti, V., S. Passaro, M. Fedi, C. Marino, S. Tamburrino, G. Ventura (2016). Sub-circular conduits and dikes offshore the Somma-Vesuvius volcano revealed by magnetic and seismic data, Geophysical Research Letters, 43(18), 9544-9551. Doi: 10.1002/2016GL070271.

Patacca, E., R. Sartori and P. Scandone, P. (1990). Tyrrhenian basin and Apenninic arcs: kinematic relations since late Tortonian times, Memorie della Società Geologica Italiana, 45, 425-451.

Porreca, M., A. Smedile, F. Speranza, T. Mochales, F. D'Ajello Caracciolo, G. Di Giulio, M. Vassallo, F. Villani, I. Nicolosi, R. Carluccio, S. Amoroso, P. Macrì, N. Buratti, F. Durante, M. Tallini and L. Sagnotti (2016). Geological reconstruction in the area of maximum co-seismic subsidence during the 2009 M_w = 6.1 L'Aquila earthquake using geophysical and borehole data. Ital. J. Geosci., 135(2), 350-362.

Porreca M., G. Minelli, M. Ercoli, A. Brobia, P. Mancinelli, F. Cruciani, C. Giorgetti, F. Carboni, F. Mirabella, G. Cavinato, A. Cannata, C. Pauselli and M.R. Barchi (2018). Seismic reflection profiles and subsurface geology of the area interested by the 2016-2017 earthquake sequence (Central Italy). Tectonics, 37(4), 1116-1137. Doi: 10.1002/2017TC004915.

Pierantoni, P., G. Deiana, and S. Galdenzi (2013). Stratigraphic and structural features of the Sibillini Mountains (Umbria-Marche Apennines, Italy). Italian Journal of Geosciences, 132(3), 497-520.

Pischiutta, M., M. Fondriest, M. Demurtas, F. Magnoni, G. Di Toro and A. Rovelli (2017). Structural control on the directional amplification of seismic noise (Campo Imperatore, central Italy). Earth and Planetary Science Letters, 471, 10-18. Doi: 10.1016/j.epsl.2017.04.017.

Pizzi, A., F. Calamita, M. Coltorti, and P. Pieruccini (2002). Quaternary normal faults, intramontane basins and seismicity in the Umbria-Marche-Abruzzi Apennine Ridge (Italy): contribution of neotectonic analysis to seismic hazard assessment, Boll. Soc. Geol. It., Spec. Issue 1, 923-929.

Pizzi, A., and F. Galadini (2009). Pre-existing cross-structures and active fault segmentation in the northern-central Apennines (Italy). Tectonophysics, 476(1), 304-319.

Pucci, S., P.M. De Martini, R. Civico, F. Villani, R. Nappi, T. Ricci, R. Azzaro, C. A. Brunori, M. Caciagli, F. R. Cinti, V. Sapia, R. De Ritis, F. Mazzarini, S. Tarquini, G. Gaudiosi, R. Nave, G. Alessio, A. Smedile, L. Alfonsi, L. Cucci and D. Pantosti (2017). Coseismic ruptures of the 24 August 2016, M_w 6.0 Amatrice earthquake (central Italy). Geophysical Research. Letters, 44. Doi:10.1002/2016GL071859.

Rovida, A., M. Locati, R. Camassi, B. Lolli and P. Gasperini (2016). CPTI15, the 2015 version of the Parametric Catalogue of Italian Earthquakes. Istituto Nazionale di Geofisica e Vulcanologia, Doi: 10.6092/INGV.IT-CPTI15.

Roberts G.P. and A.M. Michetti (2004). Spatial and temporal variations in growth rates along active normal fault Systems: an example from the Lazio-Abruzzo Apennines, central Italy, Journal of Structural Geology, 26, 339-376.

Tavarnelli, E., R.W.H. Butler, F.A. Decandia, F. Calamita, M. Grasso, W. Alvarez and P. Renda (2004). Implications of fault reactivation and structural inheritance in the Cenozoic tectonic evolution of Italy. The Geology of Italy, Special, 1, 209-222.

Walters R.J., L. C. Gregory, L. Wedmore, T. J. Craig, K. McCaffrey, M. Wilkinson, J. Chen, Z. Li, J. R. Elliott, H. Goodall, F. Iezzi, F. Livio, A. M. Michetti, G. Roberts, and E. Vittori (2018). Dual control of fault intersections on stop-start rupture in the 2016 Central Italy seismic sequence, 2018, Earth and Planetary Science Letters, 500, 1-14. Doi:10.1016/j.epsl.2018.07.043

Xu, S., E. Fukuyama, Y. Ben-Zion, and J.P. Ampuero (2016). Dynamic rupture activation of backthrust fault branching. Tectonophysics, 644-645, 161-183. Doi: 10.1016/j.tecto.2015.01.011.

*CORRESPONDING AUTHOR: Valeria PAOLETTI,
University Federico II, Department of Earth,
Environmental and Resources Sciences,
Napoli, Italy
email: paoletti@unina.it